

Online Learning Via Regularized Frequent Directions

Luo Luo, Cheng Chen

{ricky, jack_chen1990@sjtu.edu.cn}@sjtu.edu.cn
Department of Computer Science and Engineering
Shanghai Jiao Tong University

Zhihua Zhang

zhzhang@math.pku.edu.cn
School of Mathematical Sciences
Peking University

Wu-Jun Li

liwujun@nju.edu.cn
National Key Laboratory for Novel Software Technology
Collaborative Innovation Center of Novel Software Technology and Industrialization
Department of Computer Science and Technology
Nanjing University

April 25, 2017

Abstract

Online Newton step algorithms usually achieve good performance with less training samples than first order methods, but require higher space and time complexity in each iteration. In this paper, we develop a new sketching strategy called regularized frequent direction (RFD) to improve the performance of online Newton algorithms. Unlike the standard frequent direction (FD) which only maintains a sketching matrix, the RFD introduces a regularization term additionally. The regularization provides an adaptive stepsize for update, which makes the algorithm more stable. The RFD also reduces the approximation error of FD with almost the same cost and makes the online learning more robust to hyperparameters. Empirical studies demonstrate that our approach outperforms state-of-the-art second order online learning algorithms.

1. Introduction

Online learning is a typical approach for making an algorithm scalable, which constructs a learner incrementally from a sequence of examples. The online Newton step algorithm is the online analogue of the Newton-Raphson method [1, 2, 3], which incorporates the gradient information in earlier iterations. Compared with first order methods, the online Newton step algorithm has logarithmic regret bound without requirement of strongly convex assumption on loss function. Also, it needs less iterations than first order methods for the same prediction error. However, the online Newton step algorithm require quadratical space and time with respect to the number of dimensions, which is expensive for large scale problems.

In a recent study, Luo et al. [4] proposed sketched online Newton (SON) algorithms to accelerate second order online learning methods. The authors discussed several sketching strategies [5]

for approximating the second order information, including random projection [6, 7, 8], frequent direction [9, 10] and Oja’s algorithm [11, 12]. The SON achieves regret bounds nearly as good as the standard online Newton algorithms and performs well in real applications.

In this paper, we improve the SON methods with a novel sketching methods that we call regularized frequent directions (RFD). The RFD is a variant of frequent direction (FD) [9, 10], but reduces half of the approximation error bound with almost the same computational cost. Rather than approximating the matrix with a low-rank structure, RFD introduces an additional regularization term. Note that Zhang [13] proposed matrix ridge approximation (MRA) to a positive semi-definite matrix by the similar idea with RFD. However, there are two main differences between RFD and MRA. First, RFD is designed to the case that data samples come sequentially, while MRA relies on the whole dataset. Hence RFD is more suitable to online learning. Second, MRA aims to minimize the approximation error with respect to the Frobenius norm while RFD tries to minimize the spectral norm of the approximation error. In general, the spectral norm error bounds is more meaningful than the Frobenius norm [14].

In contrast to existing online Newton algorithms which usually use a fixed regularization term for each update, RFD provides an adaptive way to compute this term. This strategy achieves comparable regret bound with existing sketched online Newton methods, but makes the algorithm less sensitive to the hyperparameter.

The remainder of the paper is organized as follows. Firstly, we review the background of second order online learning and its sketched variants. Then we propose our regularized frequent direction (RFD) method with applications in online learning and provide some related theoretical analysis. Finally, we demonstrate empirical comparisons with baselines on several real-world datasets to show the superiority of our algorithms.

2. Online Learning by Sketching

In this section, we first describe the setup of convex online learning and some classical algorithms. Then we introduce the connection between online learning and sketching second order methods.

2.1 Convex Online Learning

Online learning is performed in a sequence of consecutive rounds [15]. We consider the problem of online optimization as follows. For a sequence of examples $\{\mathbf{x}^{(t)} \in \mathbb{R}^d\}$, and convex smooth loss functions $\{f_t : \mathcal{K}_t \rightarrow \mathbb{R}\}$ where the $f_t(\mathbf{w}) \triangleq \ell_t(\mathbf{w}^\top \mathbf{x}^{(t)})$ and the $\mathcal{K}_t \subset \mathbb{R}^d$ are convex compact set, the learner must decide a predictor $\mathbf{w}^{(t)}$ and suffers loss $f_t(\mathbf{w}^{(t)})$ for the t -th round. The regret at round T is then defined as:

$$R_T(\mathbf{w}^*) = \sum_{t=1}^T f_t(\mathbf{w}^{(t)}) - \sum_{t=1}^T f_t(\mathbf{w}^*),$$

where $\mathbf{w}^* = \operatorname{argmin}_{\mathbf{w} \in \mathcal{K}} \sum_{t=1}^T f_t(\mathbf{w})$ and $\mathcal{K} = \bigcap_{t=1}^T \mathcal{K}_t$.

We make the following assumptions on the loss functions [4].

Assumption 1 *The loss function ℓ_t satisfies $|\ell'_t(z)| \leq L$ whenever $|z| \leq C$, where L and C are positive constant scalars.*

Assumption 2 *There exists a $\mu_t \geq 0$ such that for all $\mathbf{u}, \mathbf{w} \in \mathcal{K}$, we have*

$$f_t(\mathbf{w}) \geq f_t(\mathbf{u}) + \nabla f_t(\mathbf{u})^\top (\mathbf{w} - \mathbf{u}) + \frac{\mu_t}{2} (\nabla f_t(\mathbf{u})^\top (\mathbf{w} - \mathbf{u}))^2.$$

Note that for bounded diameter of the domain and gradient, holding Assumption 2 only requires the exp-concave property of f_t , which is more general than strong convexity [3].

One typical online learning algorithm is online gradient descent (OGD) [2, 16]. At round $t + 1$, OGD exploits the following update rule:

$$\begin{aligned} \mathbf{u}^{(t+1)} &= \mathbf{w}^{(t)} - \beta_t \mathbf{g}^{(t)}, \\ \mathbf{w}^{(t+1)} &= \operatorname{argmin}_{\mathbf{w} \in \mathcal{K}_t} \|\mathbf{w} - \mathbf{u}^{(t+1)}\|, \end{aligned}$$

where $\mathbf{g}^{(t)} = \nabla f_t(\mathbf{w}^{(t)})$ and β_t is the stepsize. The algorithm has linear computation cost and achieves $\mathcal{O}(\frac{L^2}{H} \log T)$ regret bound for the H -strongly convex loss.

In this paper, we are more interested in online Newton step algorithms [2, 4]. The notation \mathbf{H} -norm for given positive definite matrix $\mathbf{H} \in \mathbb{R}^{d \times d}$ and vector $\mathbf{z} \in \mathbb{R}^d$ is defined as $\|\mathbf{z}\|_{\mathbf{H}} = \sqrt{\mathbf{z}^\top \mathbf{H} \mathbf{z}}$. The standard online Newton step keeps the curvature information in the matrix $\mathbf{H}^{(t)} \in \mathbb{R}^{d \times d}$ sequentially and iterates as follows:

$$\begin{aligned} \mathbf{u}^{(t+1)} &= \mathbf{w}^{(t)} - \beta_t (\mathbf{H}^{(t)})^{-1} \mathbf{g}^{(t)}, \\ \mathbf{w}^{(t+1)} &= \operatorname{argmin}_{\mathbf{w} \in \mathcal{K}_t} \|\mathbf{w} - \mathbf{u}^{(t+1)}\|_{\mathbf{H}^{(t)}}. \end{aligned} \quad (1)$$

The matrix $\mathbf{H}^{(t)}$ is constructed by the outer product of historical gradients [4, 17]:

$$\mathbf{H}^{(t)} = \alpha_0 \mathbf{I} + \sum_{i=1}^t \mathbf{g}^{(i)} (\mathbf{g}^{(i)})^\top, \quad \text{or} \quad \mathbf{H}^{(t)} = \alpha_0 \mathbf{I} + \sum_{i=1}^t (\mu_t + \eta_t) \mathbf{g}^{(i)} (\mathbf{g}^{(i)})^\top, \quad (2)$$

where $\alpha_0 \geq 0$ is a fixed regularization parameter, μ_t is the constant in Assumption 2 and η_t is a learning rate which is typically chosen by $\mathcal{O}(1/t)$. The second order algorithms enjoy logarithmical regret bound without the strongly convex assumption but require quadratical space and computation cost.

2.2 Efficient Algorithms by Sketching

To make the online Newton step scalable, it is natural to use sketching techniques [5]. Since the matrix $\mathbf{H}^{(t)}$ in online learning has the form $\mathbf{H}^{(t)} = \alpha_0 \mathbf{I} + (\mathbf{A}^{(t)})^\top \mathbf{A}^{(t)}$, where $\mathbf{A}^{(t)} \in \mathbb{R}^{t \times d}$ is the corresponding term in (2) such as

$$\mathbf{A}^{(t)} = [\mathbf{g}^{(1)}, \dots, \mathbf{g}^{(t)}]^\top, \quad \text{or} \quad \mathbf{A}^{(t)} = [\sqrt{\mu_1 + \eta_1} \mathbf{g}^{(1)}, \dots, \sqrt{\mu_t + \eta_t} \mathbf{g}^{(t)}]^\top.$$

The sketching algorithm employs an approximation of $\mathbf{A}^{(t)}$ by $\mathbf{B}^{(t)} \in \mathbb{R}^{m \times d}$ where $m \ll d$. Then we can use $\alpha_0 \mathbf{I} + (\mathbf{B}^{(t)})^\top \mathbf{B}^{(t)}$ to replace $\mathbf{H}^{(t)}$ in update (1). By the Woodbury identity formula, we can reduce the computation of the update from $\mathcal{O}(d^2)$ to $\mathcal{O}(m^2 d)$. There are several choices of sketching techniques, such as random projection [6, 7, 8], frequent direction [9, 10] and Oja's algorithm [11, 12]. Luo et al. [4] discussed how to improve online learning by these

techniques. In practice, the performance of sketched online Newton methods is sensitive to the choice of hyperparameter α_0 and they only achieve good result when α_0 is set appropriately.

We now give a brief review of frequent directions (FD) [9, 10], because it is closely related to our proposed method. Frequent Directions is a deterministic matrix sketching in the row-updates model. For any input matrix $\mathbf{A} \in \mathbb{R}^{T \times d}$ which comes from sequentially row by row, it maintains a sketch matrix $\mathbf{B} \in \mathbb{R}^{m \times d}$ to approximate $\mathbf{A}^\top \mathbf{A}$ by $\mathbf{B}^\top \mathbf{B}$. FD has following properties for any $k < m$,

$$\mathbf{A}^\top \mathbf{A} - \mathbf{B}^\top \mathbf{B} \succeq \mathbf{0}, \quad (3)$$

$$\|\mathbf{A}^\top \mathbf{A} - \mathbf{B}^\top \mathbf{B}\|_2 \leq \sum_{i=1}^{T-1} (\sigma_m^{(i)})^2 \leq \frac{1}{m-k} \|\mathbf{A} - \mathbf{A}_k\|_F^2, \quad (4)$$

where $\|\cdot\|_2$ denotes the spectral norm of the matrix and \mathbf{A}_k is the best rank- k approximation to \mathbf{A} in both the Frobenius and spectral norms.

We present the detailed implementation of FD in Algorithm 1, where $\sigma_m^{(t-1)}$ is the m -th largest singular values of $\mathbf{B}^{(t-1)}$. The dominated computation of the algorithm is computation of $\text{svd}(\mathbf{B}^{(t)})$ which requires $\mathcal{O}(m^2d)$ by the standard SVD implementation, while one can reduce the total cost from $\mathcal{O}(Tm^2d)$ into $\mathcal{O}(Tmd)$ by doubling the space [5, 9] as in Algorithm 2.

Algorithm 1 Frequent Directions

- 1: **Input:** $\mathbf{A} = [\mathbf{a}^{(1)}, \dots, \mathbf{a}^{(T)}]^\top \in \mathbb{R}^{T \times d}$, $\mathbf{B}^{(0)} = \mathbf{0}^{m \times d}$
 - 2: **for** $t = 1, \dots, T$ **do**
 - 3: Insert $(\mathbf{a}^{(t)})^\top$ into the m -th row of $\mathbf{B}^{(t-1)}$
 - 4: $[\mathbf{U}^{(t-1)}, \boldsymbol{\Sigma}^{(t-1)}, \mathbf{V}^{(t-1)}] = \text{svd}(\mathbf{B}^{(t-1)})$
 - 5: $\mathbf{B}^{(t)} = \sqrt{(\boldsymbol{\Sigma}^{(t-1)})^2 - (\sigma_m^{(t-1)})^2 \mathbf{I}} \cdot (\mathbf{V}^{(t-1)})^\top$
 - 6: **end for**
 - 7: **Output:** $\mathbf{B} = \mathbf{B}^{(T)}$
-

3. Regularized Frequent Directions

Sketching usually leads to a low-rank matrix. To make the matrix $\mathbf{H}^{(t)}$ invertible and well-conditioned, both the standard online Newton and sketched online Newton methods usually require a fixed regularization term $\alpha_0 \mathbf{I}$. The hyperparameter α_0 typically needs to be tuned manually. On the other hand, the conventional sketching algorithms such as frequent direction only consider the gradient part $(\mathbf{A}^{(t)})^\top \mathbf{A}^{(t)}$ in $\mathbf{H}^{(t)}$ and do not cover the regularization term. Intuitively, it is better to increase the factor of the identity matrix as iteration goes because there are more and more rows of $\mathbf{A}^{(t)}$. These motivate us to propose a new sketching algorithm that is more suitable to online learning.

3.1 The Algorithm

The regularized frequent direction (RFD) is a variant of frequent direction. For a given matrix $\mathbf{A} \in \mathbb{R}^{T \times d}$ whose rows come from sequentially and a fixed scalar $\alpha_0 \in \mathbb{R}$, RFD computes the sketch matrix $\mathbf{B} \in \mathbb{R}^{m \times d}$ and $\alpha \in \mathbb{R}$ ($m \ll d$) to approximate $\alpha_0 \mathbf{I} + \mathbf{A}^\top \mathbf{A}$ by $\alpha \mathbf{I} + \mathbf{B}^\top \mathbf{B}$.

Algorithm 2 Fast Frequent Directions

```

1: Input:  $\mathbf{A} = [\mathbf{a}^{(1)}, \dots, \mathbf{a}^{(T)}]^\top \in \mathbb{R}^{T \times d}$ ,  $\mathbf{B}^{(0)} = \mathbf{0}^{2m \times d}$ 
2: for  $t = 1, \dots, T$  do
3:   Insert  $(\mathbf{a}^{(t)})^\top$  into a zero-valued row of  $\mathbf{B}^{(t-1)}$ 
4:   if  $\mathbf{B}^{(t-1)}$  has no zero-valued row
5:      $[\mathbf{U}^{(t-1)}, \mathbf{\Sigma}^{(t-1)}, \mathbf{V}^{(t-1)}] = \text{svd}(\mathbf{B}^{(t-1)})$ 
6:      $\mathbf{B}^{(t)} = \sqrt{(\mathbf{\Sigma}^{(t-1)})^2 - (\sigma_m^{(t-1)})^2 \mathbf{I}} \cdot (\mathbf{V}^{(t-1)})^\top$ 
7:   else
8:      $\mathbf{B}^{(t)} = \mathbf{B}^{(t-1)}$ 
9:   end if
10: end for
11: Output:  $\mathbf{B} = \mathbf{B}^{(T)}$ 
    
```

Algorithm 3 Regularized Frequent Directions

```

1: Input:  $\mathbf{A} = [\mathbf{a}^{(1)}, \dots, \mathbf{a}^{(T)}]^\top \in \mathbb{R}^{T \times d}$ ,  $\mathbf{B}^{(0)} = \mathbf{0}^{m \times d}$ ,  $\alpha^{(0)} = \alpha_0 \in \mathbb{R}$ 
2: for  $i = 1, \dots, T$  do
3:   Insert  $(\mathbf{a}^{(t)})^\top$  into a zero-valued row of  $\mathbf{B}^{(t-1)}$ 
4:    $[\mathbf{U}^{(t-1)}, \mathbf{\Sigma}^{(t-1)}, \mathbf{V}^{(t-1)}] = \text{svd}(\mathbf{B}^{(t-1)})$ 
5:    $\mathbf{B}^{(t)} = \sqrt{(\mathbf{\Sigma}^{(t-1)})^2 - (\sigma_m^{(t-1)})^2 \mathbf{I}} \cdot (\mathbf{V}^{(t-1)})^\top$ 
6:    $\alpha^{(t)} = \alpha^{(t-1)} + (\sigma_m^{(t-1)})^2 / 2$ 
7: end for
8: Output:  $\mathbf{B} = \mathbf{B}^{(T)}$  and  $\alpha = \alpha^{(T)}$ .
    
```

We demonstrate the detailed implementation of RFD in Algorithm 3. Compared with the standard FD, RFD only maintains an extra variable $\alpha^{(t)}$ by scalar operations for each iteration, hence the cost of RFD is almost the same as FD. In real applications, $\alpha^{(t)}$ is typically increasing as iteration from the $(m+1)$ -th round, which makes $\alpha \mathbf{I} + \mathbf{B}^\top \mathbf{B}$ positive definite even the initial $\alpha^{(0)}$ is zero. Also, we can further accelerate it by doubling the space as shown in Algorithm 4.

3.2 Theoretical Analysis

We now explain why the regularization term is updated by the rule of Algorithm 3 and provide the approximation error bound of RFD. Firstly, we give the following theorem about matrix approximation.

Theorem 1 *Given a positive semi-definite matrix $\mathbf{M} \in \mathbb{R}^{d \times d}$ and a positive integer $k < d$, let $\mathbf{M} = \mathbf{U}\mathbf{\Sigma}\mathbf{U}^\top$ be the SVD of \mathbf{M} . Let \mathbf{U}_k denote the matrix of the first k columns of \mathbf{U} and σ_k be the top k -th singular value of \mathbf{M} . Then the pair $(\hat{\mathbf{C}}, \hat{\delta})$, defined as*

$$\hat{\mathbf{C}} = \mathbf{U}_k(\mathbf{\Sigma}_k - \hat{\delta}\mathbf{I})^{1/2}\mathbf{V} \quad \text{and} \quad \hat{\delta} = (\sigma_{k+1} + \sigma_d)/2$$

Algorithm 4 Fast Regularized Frequent Directions

```

1: Input:  $\mathbf{A} = [\mathbf{a}^{(1)}, \dots, \mathbf{a}^{(T)}]^\top \in \mathbb{R}^{T \times d}$ ,  $\mathbf{B}^{(0)} = \mathbf{0}^{2m \times d}$ ,  $\alpha^{(0)} = \alpha_0 \in \mathbb{R}$ 
2: for  $t = 1, \dots, T$  do
3:   Insert  $(\mathbf{a}^{(t)})^\top$  into a zero-valued row of  $\mathbf{B}^{(t-1)}$ 
4:   if  $\mathbf{B}^{(t-1)}$  has no zero-valued row
5:      $[\mathbf{U}^{(t-1)}, \mathbf{\Sigma}^{(t-1)}, \mathbf{V}^{(t-1)}] = \text{svd}(\mathbf{B}^{(t-1)})$ 
6:      $\mathbf{B}^{(t)} = \sqrt{(\mathbf{\Sigma}^{(t-1)})^2 - (\sigma_m^{(t-1)})^2 \mathbf{I}} \cdot (\mathbf{V}^{(t-1)})^\top$ 
7:      $\alpha^{(t)} = \alpha^{(t-1)} + (\sigma_m^{(t-1)})^2 / 2$ 
8:   else
9:      $\mathbf{B}^{(t)} = \mathbf{B}^{(t-1)}$ 
10:  end if
11: end for
12: Output:  $\mathbf{B} = \mathbf{B}^{(T)}$ 
    
```

where \mathbf{V} is an arbitrary $k \times k$ orthonormal matrix, is the global minimizer of

$$\min_{\mathbf{C} \in \mathbb{R}^{d \times k}, \delta \in \mathbb{R}} \|\mathbf{M} - \mathbf{C}\mathbf{C}^\top - \delta \mathbf{I}\|_2.$$

Theorem 1 provides the closed form optimal solution for matrix approximation with regularization term. Zhang [13] has established the Frobenius norm based result in optimization view, while our analysis relies on the properties of unitary invariant norms. Moreover, our derivation is more concise. Additionally, we prove the solution is global optimal while Zhang's analysis is local (see Appendix A).

At the t -th round, our goal is to approximate the concentration of historical approximation and current data. The following theorem shows that our update is optimal with respect to the spectral norm.

Theorem 2 *Based on the updates in Algorithm 3 and letting $\mathbf{B}^{(t)}$ refer to the matrix obtained by Line 5 of Algorithm 3 at the t -th iteration (without inserting $\mathbf{a}^{(t)}$ in the next iteration), and $\tilde{\mathbf{B}}^{(t)}$ be the matrix consists of the first $m - 1$ rows of $\mathbf{B}^{(t)}$, we have*

$$(\tilde{\mathbf{B}}^{(t)}, \alpha^{(t)}) = \underset{\substack{\tilde{\mathbf{B}} \in \mathbb{R}^{d \times (m-1)}, \\ \alpha \in \mathbb{R}}}{\text{argmin}} \|\alpha^{(t-1)} \mathbf{I} + (\mathbf{B}^{(t-1)})^\top \mathbf{B}^{(t-1)} - \tilde{\mathbf{B}}^\top \tilde{\mathbf{B}} - \alpha \mathbf{I}\|_2. \quad (5)$$

Theorem 2 provides a natural explanation to RFD, making the algorithm reasonable intuitively, while the standard FD sketching is only an extension of approximating item frequencies in streams [18] but lacks optimization view in the matrix case.

RFD also enjoys a tighter approximation error shown in the following theorem.

Theorem 3 *For any $k < m$ and using the notation of Algorithm 3, we have*

$$\|\mathbf{A}^\top \mathbf{A} - (\mathbf{B}^\top \mathbf{B} + \alpha \mathbf{I})\|_2 \leq \frac{1}{2(m-k)} \|\mathbf{A} - \mathbf{A}_k\|_F^2, \quad (6)$$

where \mathbf{A}_k is the best rank- k approximation to \mathbf{A} in both the Frobenius and spectral norm.

The right-hand side of inequality (6) is the half of the one in (4), which means RFD reduces the approximation error significantly with only one extra scalar.

The approximation Hessian of sketched online Newton step typically has a regularization term. Hence we are more interested in approximating the matrix that can be expressed as $\mathbf{M} = \alpha_0 \mathbf{I} + \mathbf{A}^\top \mathbf{A}$ where $\alpha_0 > 0$. Suppose that the standard FD approximates $\mathbf{A}^\top \mathbf{A}$ by $\mathbf{B}^\top \mathbf{B}$. Then it estimates \mathbf{M} as $\mathbf{M}_{\text{FD}} = \alpha_0 \mathbf{I} + \mathbf{B}^\top \mathbf{B}$, but RFD uses $\mathbf{M}_{\text{RFD}} = \alpha \mathbf{I} + \mathbf{B}^\top \mathbf{B}$. Theorem 4 shows that \mathbf{M}_{RFD} is well-conditioned no worse than \mathbf{M}_{FD} and \mathbf{M} . In general, the equality in the theorem usually can not be hold for $t > m$ unless $(\mathbf{a}^{(t)})^\top$ lies in the row space of $\mathbf{B}^{(t-1)}$ exactly or the first t rows of \mathbf{A} have perfect low rank structure, which means that RFD results in a well-conditioned approximation more than others in practice.

Theorem 4 *With the notation of Algorithms 1 and 3, let $\mathbf{M} = \alpha_0 \mathbf{I} + \mathbf{A}^\top \mathbf{A}$, $\mathbf{M}_{\text{FD}} = \alpha_0 \mathbf{I} + \mathbf{B}^\top \mathbf{B}$ and $\mathbf{M}_{\text{RFD}} = \alpha \mathbf{I} + \mathbf{B}^\top \mathbf{B}$, where $\alpha_0 > 0$ is a fixed scalar. Define the condition number of any nonsingular matrix \mathbf{H} as $\kappa(\mathbf{H}) = \sigma_{\max}(\mathbf{H})/\sigma_{\min}(\mathbf{H})$, where $\sigma_{\max}(\mathbf{H})$ and $\sigma_{\min}(\mathbf{H})$ are the largest and smallest singular values of \mathbf{H} respectively. Then we have $\kappa(\mathbf{M}_{\text{RFD}}) \leq \kappa(\mathbf{M}_{\text{FD}})$ and $\kappa(\mathbf{M}_{\text{RFD}}) \leq \kappa(\mathbf{M})$.*

4. The Online Newton Step by RFD

We now present the online Newton step by Regularized frequent directions (RFD-SON). The procedure is shown in Algorithm 5, which is similar to sketched online Newton step (SON) [4] but with the new sketching method RFD.

Algorithm 5 RFD for Online Newton Step

- 1: **Input:** $\alpha^{(0)} = \alpha_0$, $m < d$, $\eta_t = \mathcal{O}(1/t)$ and $\mathbf{B}^{(0)} = \mathbf{0}^{m \times d}$.
 - 2: **for** $t = 1, \dots, T$ **do**
 - 3: Receive example $\mathbf{x}^{(t)}$, and loss function $f_t(\mathbf{w})$
 - 4: $\mathbf{g}^{(t)} = \nabla f_t(\mathbf{w}^{(t)})$
 - 5: Insert $(\sqrt{\mu_t + \eta_t} \mathbf{g}^{(t)})^\top$ into the m -th row of $\mathbf{B}^{(t-1)}$
 - 6: $[\mathbf{U}^{(t-1)}, \mathbf{\Sigma}^{(t-1)}, \mathbf{V}^{(t-1)}] = \text{svd}(\mathbf{B}^{(t-1)})$
 - 7: $\mathbf{B}^{(t)} = \sqrt{(\mathbf{\Sigma}^{(t-1)})^2 - (\sigma_m^{(t-1)})^2} \mathbf{I} \cdot (\mathbf{V}^{(t-1)})^\top$
 - 8: $\alpha^{(t)} = \alpha^{(t-1)} + (\sigma_m^{(t-1)})^2 / 2$
 - 9: $\mathbf{H}^{(t)} = \alpha^{(t)} \mathbf{I} + (\mathbf{B}^{(t)})^\top \mathbf{B}^{(t)}$
 - 10: $\mathbf{u}^{(t+1)} = \mathbf{w}^{(t)} - (\mathbf{H}^{(t)})^{-1} \mathbf{g}^{(t)}$
 - 11: $\mathbf{w}^{(t+1)} = \text{argmin}_{\mathbf{w} \in \mathcal{K}_t} \|\mathbf{w} - \mathbf{u}^{(t+1)}\|_{\mathbf{H}^{(t)}}$
 - 12: **end for**
-

Theorem 5 Let $\mu = \max_{t=1}^T \{\mu_t\}$ and $\mathcal{K} = \bigcap_{t=1}^T \mathcal{K}_t$. Then under Assumptions 1 and 2 for any $\mathbf{w} \in \mathcal{K}$, Algorithm 5 has the following regret

$$R_T(\mathbf{w}) \leq \frac{\alpha_0}{2} \|\mathbf{w}\|^2 + 2(CL)^2 \sum_{t=1}^T \eta_t + \frac{m}{2(\mu + \eta_T)} \ln \left(\text{tr}((\mathbf{B}^{(T)})^\top \mathbf{B}^{(T)}) + \frac{\alpha^{(T)}}{\alpha_0} \right) + \Omega_{\text{RFD}} \quad (7)$$

where

$$\Omega_{\text{RFD}} = \frac{d-m}{2(\mu + \eta_T)} \ln \frac{\alpha^{(T)}}{\alpha_0} + \frac{m}{4(\mu + \eta_T)} \sum_{t=1}^T \frac{(\sigma_m^{(t)})^2}{\alpha^{(t)}} + C^2 \sum_{t=1}^T (\sigma_m^{(t-1)})^2.$$

We present the regret bound of RFD-SON in Theorem 5. The last term in (7) is the main gap between RFD-SON and the standard online Newton step without sketching, and the terms are logarithmic to T . Ω_{RFD} is dominated by the last term which can be bounded as (4). If we exploit the standard FD to sketched online Newton step [4] (RFD-SON), the gap will be

$$\Omega_{\text{FD}} = \frac{m}{2(\mu + \eta_T)} \sum_{t=1}^T \frac{(\sigma_m^{(t-1)})^2}{\alpha_0},$$

which looks comparable to our result because it is also dependent on $\sum_{t=1}^T (\sigma_m^{(t-1)})^2$. However, The bound of FD-SON is highly related to the hyperparameter α_0 . If we increase the value of α_0 , the gap Ω_{FD} can be reduced, but the term $\frac{\alpha_0}{2} \|\mathbf{w}\|^2$ will increase. For RFD-SON, we can set α_0 be sufficient small to reduce $\frac{\alpha_0}{2} \|\mathbf{w}\|^2$ and it affects the term Ω_{RFD} limited. The reason is that the first term of Ω_{RFD} contains $\frac{1}{\alpha_0}$ in the logarithmic term and the second term contains $\alpha^{(t)} = \alpha_0 + \frac{1}{2} \sum_{i=1}^{t-1} (\sigma_m^{(i)})^2$ in the denominator. For large t , $\alpha^{(t)}$ is mainly dependent on $\sum_{i=1}^{t-1} (\sigma_m^{(i)})^2$, rather than α_0 .

5. Experiments

In this section, we evaluate the performance of regularized frequent directions (RFD) and online Newton step by RFD (RFD-SON) on three real-world datasets ‘‘a9a’’, ‘‘gisette’’ and ‘‘sido0’’ whose details are listed in Table 1. The ‘‘sido0’’ dataset comes from Causality Workbench¹ and the others can be downloaded from LIBSVM repository². The experiments are conducted in Matlab and run on a server with Intel (R) Core (TM) i7-3770 CPU 3.40GHz×2, 8GB RAM and Windows Server 2012 64-bit system.

Table 1: Summary of datasets used in our experiments

datasets	n	d	source
a9a	32,561	123	[19]
gisette	6,000	5,000	[20]
sido0	12,678	4,932	[21]

1. <http://www.causality.inf.ethz.ch/data/SIDO.html>

2. <https://www.csie.ntu.edu.tw/~cjlin/libsvmtools/datasets/>

5.1 Matrix Approximation

We first compare the approximation error of FD and RFD. For a given dataset $\mathbf{A} \in \mathbb{R}^{n \times d}$ of n samples with d features, we use FD (Algorithm 2) and RFD (Algorithm 4) to approximate the covariance matrix $\mathbf{A}^\top \mathbf{A}$ by $\mathbf{B}^\top \mathbf{B}$ and $\alpha \mathbf{I} + \mathbf{B}^\top \mathbf{B}$ respectively; that is,

$$\text{Error-FD} = \frac{\|\mathbf{A}^\top \mathbf{A} - \mathbf{B}^\top \mathbf{B}\|_2}{\|\mathbf{A}^\top \mathbf{A}\|_2}, \quad \text{and} \quad \text{Error-RFD} = \frac{\|\mathbf{A}^\top \mathbf{A} - \mathbf{B}^\top \mathbf{B} - \alpha \mathbf{I}\|_2}{\|\mathbf{A}^\top \mathbf{A}\|_2}.$$

The regularization term α_0 is not important for this evaluation because it does not change the absolute error in the numerator of Error-FD or Error-RFD. We report the relative spectral norm error by varying the sketch size m . Figure 1 shows the performance of the two Algorithms. The relative error of RFD is always lower than the one of FD and the decrement is nearly the half in most cases. The results match the theoretical analysis (Theorem 3) very well. We do not include the comparison of the running time because they are almost the same.

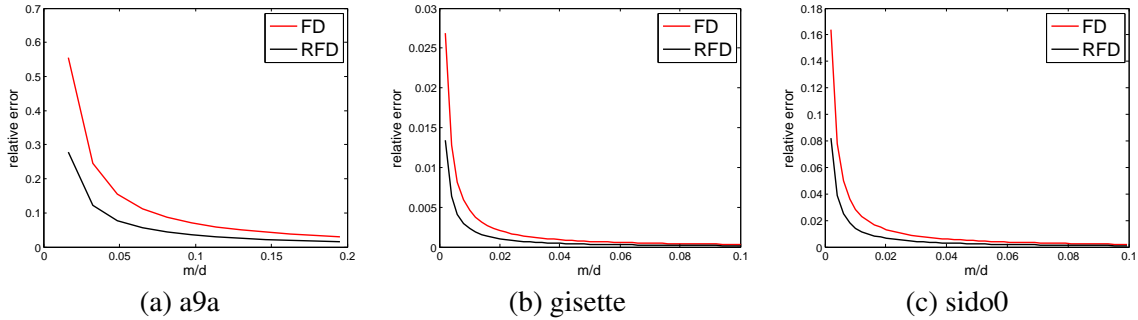


Figure 1: Comparison of relative spectral error with proportion of the sketching size

5.2 Online Learning

We now evaluate the performance of RFD-SON. We use the least squares loss (that is, $f_t(\mathbf{w}) = (\mathbf{w}^\top \mathbf{x}^{(t)} - y^{(t)})^2$), and set $\mathcal{K}_t = \{\mathbf{w} : |\mathbf{w}^\top \mathbf{x}^{(t)}| \leq 1\}$. In the experiments, we use the doubling space strategy on RFD sketching, which is shown in Algorithm 6.

By the Woodbury formula, the parameter $\mathbf{w}^{(t)}$ can be updated in $\mathcal{O}(md)$ cost as follows

$$\begin{aligned} \mathbf{u}^{(t+1)} &= \mathbf{w}^{(t)} - \frac{1}{\alpha^{(t)}} (\mathbf{g}^{(t)} - (\mathbf{B}^{(t)})^\top \mathbf{H}^{(t)} \mathbf{B}^{(t)} \mathbf{g}^{(t)}), \\ \mathbf{w}^{(t+1)} &= \mathbf{u}^{(t+1)} - \gamma^{(t)} (\mathbf{x}^{(t)} - (\mathbf{B}^{(t)})^\top \mathbf{H}^{(t)} \mathbf{B}^{(t)} \mathbf{x}^{(t)}), \end{aligned}$$

where

$$\gamma^{(t)} = \frac{\tau((\mathbf{u}^{(t)})^\top \mathbf{x}^{(t)})}{(\mathbf{x}^{(t)})^\top \mathbf{x}^{(t)} - (\mathbf{x}^{(t)})^\top (\mathbf{B}^{(t)})^\top \mathbf{H}^{(t)} \mathbf{B}^{(t)} \mathbf{x}^{(t)}} \quad \text{and} \quad \tau(z) = \text{sgn}(z) \max\{|z| - 1, 0\}.$$

The detailed derivation of the projection step can be found in Luo et al. [4].

We use 70% data for training and the rest for test. The algorithms in the experiments include ADAGRAD; standard online Newton step with the full Hessian [17] (FULL-ON); sketched online Newton step with frequent directions (FD-SON), random projections (RP-SON), Oja's algorithms

Algorithm 6 Fast RFD for Online Newton Step

```

1: Input:  $\alpha^{(0)} = \alpha_0$ ,  $m < d$ ,  $\eta_t = \mathcal{O}(1/t)$  and  $\mathbf{B}^{(0)} = \mathbf{0}^{m \times d}$ .
2: for  $t = 1, \dots, T$  do
3:   Receive example  $\mathbf{x}^{(t)}$ , and loss function  $f_t(\mathbf{w})$ 
4:    $\mathbf{g}^{(t)} = \nabla f_t(\mathbf{w}^{(t)})$ 
5:   Insert  $(\sqrt{\mu_t + \eta_t} \mathbf{g}^{(t)})^\top$  into the  $m$ -th row of  $\mathbf{B}^{(t-1)}$ 
6:   if  $\mathbf{B}^{(t-1)}$  has no zero valued rows
7:      $[\mathbf{U}^{(t-1)}, \mathbf{\Sigma}^{(t-1)}, \mathbf{V}^{(t-1)}] = \text{svd}(\mathbf{B}^{(t-1)})$ 
8:      $\mathbf{B}^{(t)} = \sqrt{(\mathbf{\Sigma}^{(t-1)})^2 - (\sigma_m^{(t-1)})^2} \mathbf{I} \cdot (\mathbf{V}^{(t-1)})^\top$ 
9:      $\alpha^{(t)} = \alpha^{(t-1)} + (\sigma_m^{(t-1)})^2 / 2$ 
10:  else
11:     $\mathbf{B}^{(t)} = \mathbf{B}^{(t-1)}$ 
12:  end if
13:   $\mathbf{H}^{(t)} = \alpha^{(t)} \mathbf{I} + (\mathbf{B}^{(t)})^\top \mathbf{B}^{(t)}$ 
14:   $\mathbf{u}^{(t+1)} = \mathbf{w}^{(t)} - (\mathbf{H}^{(t)})^{-1} \mathbf{g}^{(t)}$ 
15:   $\mathbf{w}^{(t+1)} = \text{argmin}_{\mathbf{w} \in \mathcal{K}_t} \|\mathbf{w} - \mathbf{u}^{(t+1)}\|_{\mathbf{H}^{(t)}}$ 
16: end for
    
```

(Oja-SON) [4], and our proposed sketched online Newton step with regularized frequent directions (RFD-SON). The hyperparameter α_0 is tuned from $\{10^{-10}, 10^{-9}, \dots, 10^9, 10^{10}\}$ and the sketch size for FD-SON, RP-SON, Oja-SON and RFD-SON is chosen from $\{5, 10, 20\}$.

Table 2 reports the accuracy for all the above algorithms at one epoch with the best α_0 , and Table 3 includes the corresponding running times. ADAGRAD has apparently less accuracy than the second order methods although it is the fastest. The SON methods are more efficient than FULL-ON as we expected. The costs of FD-SON and RFD-SON are not identical here because the approximation methods will generate different $\mathbf{g}^{(t)}$ at each step which makes the matrices to be estimated not same. The accuracy of RFD-SON with $m = 20$ is (one of) the best on all the datasets.

We are also interested in how the hyperparameter α_0 affects the performance of the algorithm. Figures 2, 3 and 4 show the results. We display the results of baselines when α_0 is near to the best one for all the baseline algorithms. Note that only FULL-ON is robust to the hyperparameter on “a9a” and “sido0”. In most cases, the baselines are sensitive to the choice of the hyperparameter. But the proposed RFD-SON is very robust to the hyperparameter. We demonstrate the behaviors of RFD-SON with a large range of α_0 . The algorithm typically achieves comparable good performance when α_0 is not too large (the accuracy of all the second order methods will decrease apparently when α_0 reaches 10^4). Specifically, RFD-SON with $\alpha_0 = 10^{-10}$ has almost the same performance as the best choice of the hyperparameter on “a9a” and “sido0”. RFD-SON is even more stable than the standard online Newton step algorithm. The reason is that the estimate of the Hessian in our method is typically more well-conditioned.

Table 2: Accuracy on datasets with best α_0 (%)

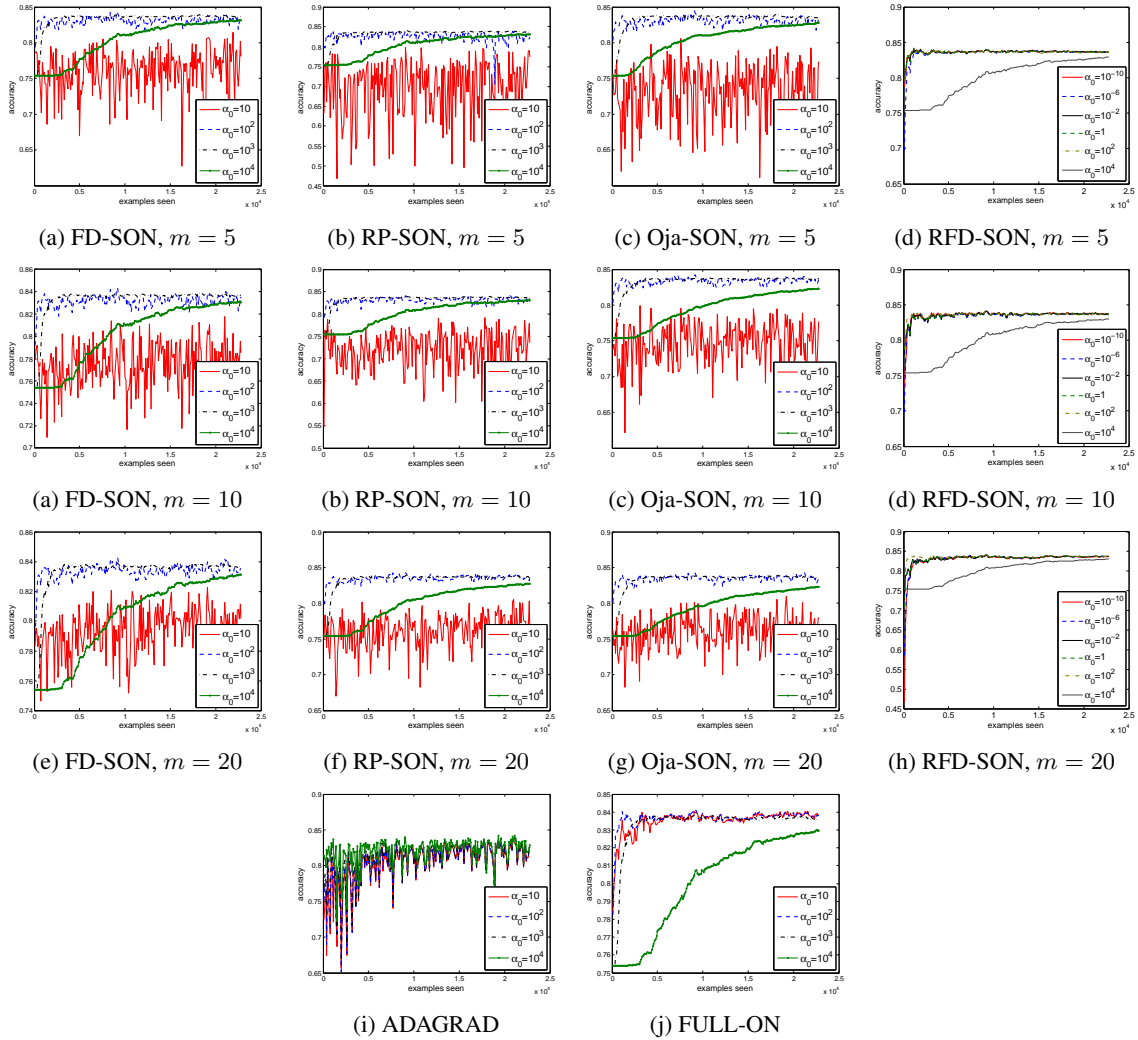
datasets	a9a	gisette	sido0
ADAGRAD	83.4783	93.9444	94.0326
FULL-ON	83.8264	96.9444	97.0557
FD-SON, $m = 5$	83.6524	96.7222	97.0557
FD-SON, $m = 10$	83.6728	96.7222	97.0557
FD-SON, $m = 20$	83.6831	96.8889	97.0820
RP-SON, $m = 5$	83.6626	96.2778	96.6614
RP-SON, $m = 10$	83.7240	96.7222	97.0294
RP-SON, $m = 20$	83.6626	96.4444	97.0820
Oja-SON, $m = 5$	83.7650	96.6111	96.7403
Oja-SON, $m = 10$	83.7547	96.7778	97.0820
Oja-SON, $m = 20$	83.6217	96.6111	97.0032
RFD-SON, $m = 5$	83.6319	96.2222	96.6877
RFD-SON, $m = 10$	83.6831	96.4444	96.9243
RFD-SON, $m = 20$	83.9390	96.9444	97.0820

Table 3: The training time on datasets with best α_0 (in second)

datasets	a9a	gisette	sido0
ADAGRAD	40.66	518.97	234.87
FULL-ON	44.62	1468.00	1770.96
FD-SON, $m = 5$	40.16	870.11	1149.54
FD-SON, $m = 10$	41.55	931.86	1347.88
FD-SON, $m = 20$	49.06	1210.65	1634.75
RP-SON, $m = 5$	17.01	822.59	1028.24
RP-SON, $m = 10$	18.04	864.76	1060.56
RP-SON, $m = 20$	21.33	953.37	1198.24
Oja-SON, $m = 5$	17.75	820.23	1006.12
Oja-SON, $m = 10$	17.43	870.78	1048.01
Oja-SON, $m = 20$	20.38	953.11	1196.61
RFD-SON, $m = 5$	35.42	879.23	1073.15
RFD-SON, $m = 10$	40.14	960.70	1227.98
RFD-SON, $m = 20$	43.33	1132.20	1569.94

6. Conclusions

In this paper, we have studied the second order online learning algorithms. We have proposed a novel sketching method regularized frequent directions (RFD) with several nice properties. Both the theoretical analysis and experiments show RFD is much better than FD. The online learning algorithm with RFD achieves better accuracy than baselines and more robust to the regularization parameters. The application of RFD is not limited to convex online optimization. We will try to exploit RFD to improve other optimization algorithms including stochastic or non-convex cases.


 Figure 2: Comparison of algorithms on “a9a” with various α_0

References

- [1] Elad Hazan and Sanjeev Arora. *Efficient algorithms for online convex optimization and their applications*. Princeton University, 2006.
- [2] Elad Hazan, Amit Agarwal, and Satyen Kale. Logarithmic regret algorithms for online convex optimization. *Machine Learning*, 69(2-3):169–192, 2007.
- [3] Elad Hazan et al. Introduction to online convex optimization. *Foundations and Trends® in Optimization*, 2(3-4):157–325, 2016.
- [4] Haipeng Luo, Alekh Agarwal, Nicolò Cesa-Bianchi, and John Langford. Efficient second order online learning by sketching. In *Advances in Neural Information Processing Systems*, pages 902–910, 2016.

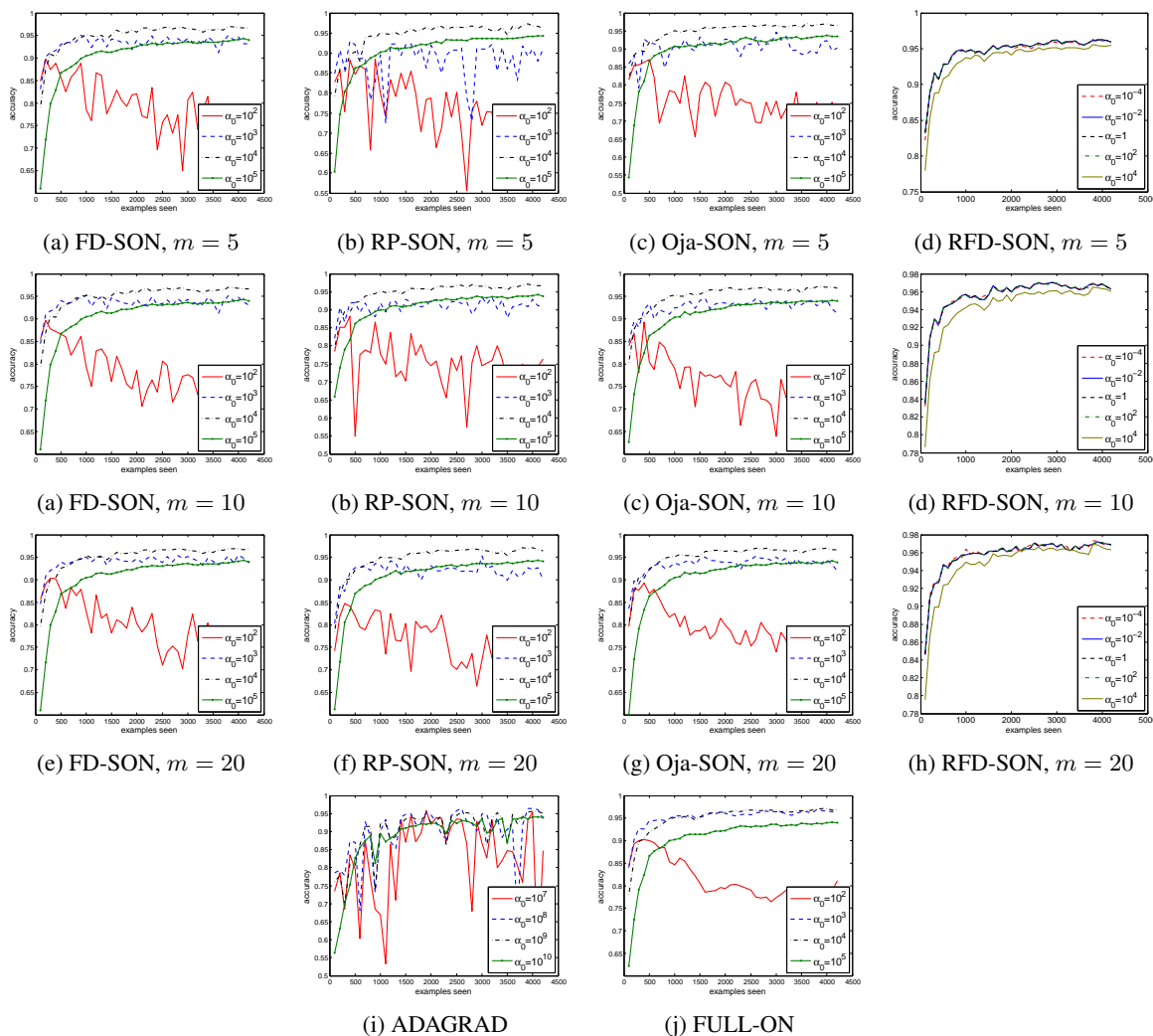
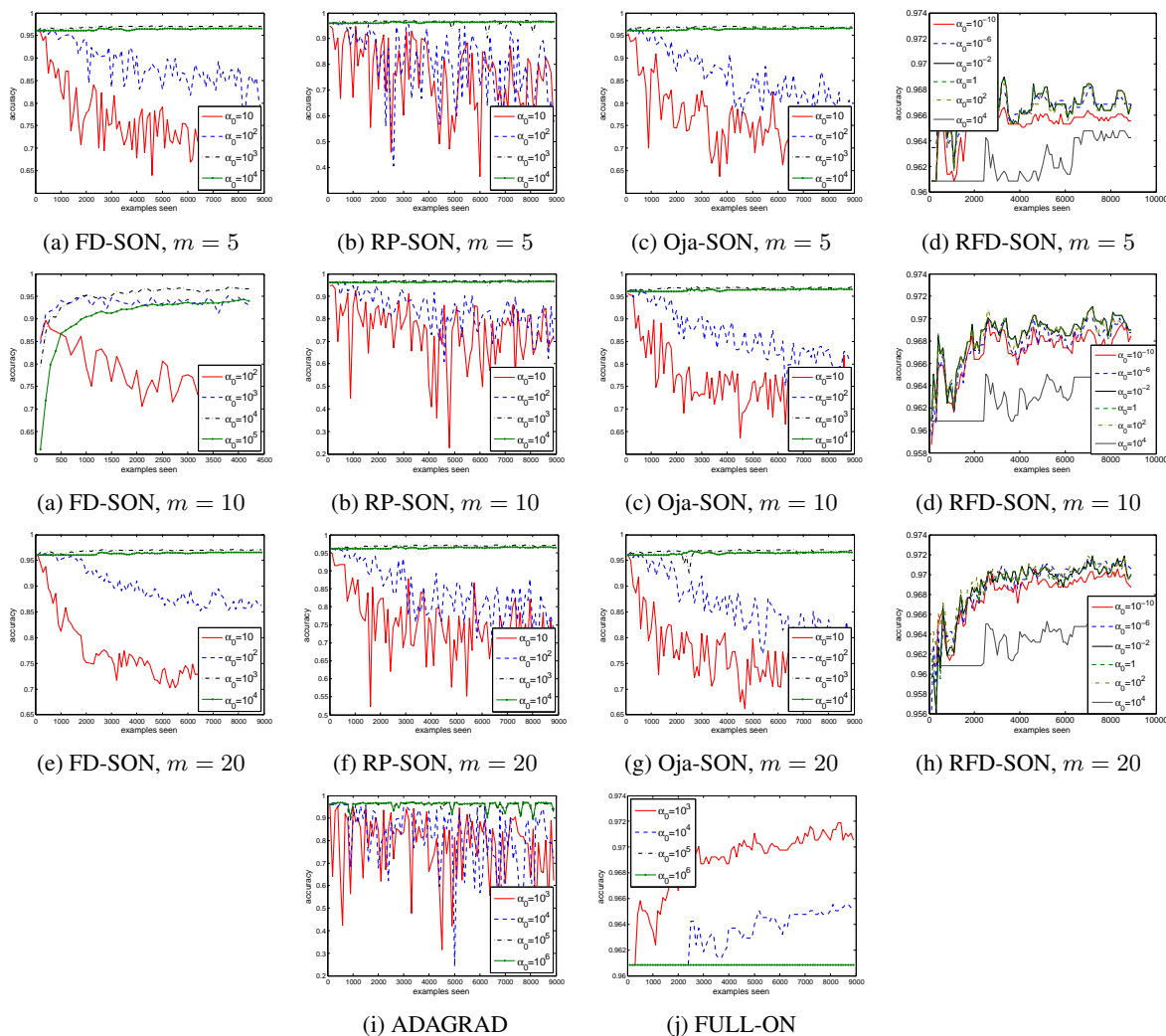


Figure 3: Comparison of algorithms on “gisette” with various α_0

- [5] David P Woodruff. Sketching as a tool for numerical linear algebra. *arXiv preprint arXiv:1411.4357*, 2014.
- [6] Piotr Indyk and Rajeev Motwani. Approximate nearest neighbors: towards removing the curse of dimensionality. In *Proceedings of the thirtieth annual ACM symposium on Theory of computing*, pages 604–613. ACM, 1998.
- [7] Dimitris Achlioptas. Database-friendly random projections: Johnson-lindenstrauss with binary coins. *Journal of computer and System Sciences*, 66(4):671–687, 2003.
- [8] Daniel M Kane and Jelani Nelson. Sparsier johnson-lindenstrauss transforms. *Journal of the ACM (JACM)*, 61(1):4, 2014.


 Figure 4: Comparison of algorithms on “sido0” with various α_0

- [9] Edo Liberty. Simple and deterministic matrix sketching. In *Proceedings of the 19th ACM SIGKDD international conference on Knowledge discovery and data mining*, pages 581–588. ACM, 2013.
- [10] Mina Ghashami, Edo Liberty, Jeff M. Phillips, and David P. Woodruff. Frequent directions: Simple and deterministic matrix sketching. *SIAM J. Comput.*, 45(5):1762–1792, 2016.
- [11] Erkki Oja. Simplified neuron model as a principal component analyzer. *Journal of mathematical biology*, 15(3):267–273, 1982.
- [12] Erkki Oja and Juha Karhunen. On stochastic approximation of the eigenvectors and eigenvalues of the expectation of a random matrix. *Journal of mathematical analysis and applications*, 106(1):69–84, 1985.

- [13] Zhihua Zhang. The matrix ridge approximation: algorithms and applications. *Machine Learning*, 97(3):227–258, 2014.
- [14] Joel A. Tropp. An introduction to matrix concentration inequalities. *Foundations and Trends in Machine Learning*, 8(1-2):1–230, 2015.
- [15] Shai Shalev-Shwartz. Online learning and online convex optimization. *Foundations and Trends in Machine Learning*, 4(2):107–194, 2011.
- [16] Martin Zinkevich. Online convex programming and generalized infinitesimal gradient ascent. 2003.
- [17] John Duchi, Elad Hazan, and Yoram Singer. Adaptive subgradient methods for online learning and stochastic optimization. *Journal of Machine Learning Research*, 12(Jul):2121–2159, 2011.
- [18] Jayadev Misra and David Gries. Finding repeated elements. *Science of computer programming*, 2(2):143–152, 1982.
- [19] John C Platt. 12 fast training of support vector machines using sequential minimal optimization. *Advances in kernel methods*, pages 185–208, 1999.
- [20] Isabelle Guyon, Steve R Gunn, Asa Ben-Hur, and Gideon Dror. Result analysis of the nips 2003 feature selection challenge. In *NIPS*, volume 4, pages 545–552, 2004.
- [21] I Guyon. Sido: A pharmacology dataset. URL: <http://www.causality.inf.ethz.ch/data/SIDO.html>, 2008.
- [22] RA Horn and CR Johnson. Topics in matrix analysis, vol. 2. *Camb. Univ. Press, England*, 1991.

Appendix A: The Proof of Theorem 1

In this section, we firstly provide several lemmas from the book “Topics in matrix analysis” [22], then we prove Theorem 1. The proof of Lemma 1 and 2 can be found in the book and we give the proof of Lemma 3 here.

Lemma 1 (Theorem 3.4.5 of [22]) *Let $\mathbf{A}, \mathbf{B} \in \mathbb{R}^{m \times n}$ be given, and suppose \mathbf{A} , \mathbf{B} and $\mathbf{A} - \mathbf{B}$ have decreasingly ordered singular values, $\sigma_1(\mathbf{A}) \geq \dots \geq \sigma_q(\mathbf{A})$, $\sigma_1(\mathbf{B}) \geq \dots \geq \sigma_q(\mathbf{B})$, and $\sigma_1(\mathbf{A} - \mathbf{B}) \geq \dots \geq \sigma_q(\mathbf{A} - \mathbf{B})$, where $q = \min\{m, n\}$. Define $s_i(\mathbf{A}, \mathbf{B}) \equiv |\sigma_i(\mathbf{A}) - \sigma_i(\mathbf{B})|$, $i = 1, \dots, q$ and let $s_{[1]}(\mathbf{A}, \mathbf{B}) \geq \dots \geq s_{[q]}(\mathbf{A}, \mathbf{B})$ denote a decreasingly ordered rearrangement of the values $s_i(\mathbf{A}, \mathbf{B})$. Then*

$$\sum_{i=1}^k s_{[i]}(\mathbf{A}, \mathbf{B}) \leq \sum_{i=1}^k \sigma_i(\mathbf{A} - \mathbf{B}) \text{ for } k = 1, \dots, q.$$

Lemma 2 (Corollary 3.5.9 of [22]) *Let $\mathbf{A}, \mathbf{B} \in \mathbb{R}^{m \times n}$ be given, and let $q = \min\{m, n\}$. The following are equivalent*

1. $\|\mathbf{A}\| \leq \|\mathbf{B}\|$ for every unitarily invariant norm $\|\cdot\|$ on $\mathbb{R}^{m \times n}$.
2. $N_k(\mathbf{A}) \leq N_k(\mathbf{B})$ for $k = 1, \dots, q$ where $N_k(\mathbf{X}) \equiv \sum_{i=1}^k \sigma_i(\mathbf{X})$ denotes by Ky Fan k -norm.

Lemma 3 (Page 215 of [22]) Let $\mathbf{A}, \mathbf{B} \in \mathbb{R}^{m \times n}$ be given, and let $q = \min\{m, n\}$. Define the diagonal matrix $\Sigma(\mathbf{A}) = [\sigma_{ij}] \in \mathbb{R}^{m \times n}$ by $\sigma_{ii} = \sigma_i(\mathbf{A})$, all other $\sigma_{ij} = 0$, where $\sigma_1(\mathbf{A}) \geq \dots \geq \sigma_q(\mathbf{A})$ are the decreasingly ordered singular values of \mathbf{A} . We define $\Sigma(\mathbf{B})$ similarly. Then we have $\|\mathbf{A} - \mathbf{B}\| \geq \|\Sigma(\mathbf{A}) - \Sigma(\mathbf{B})\|$ for every unitarily invariant norm $\|\cdot\|$.

Proof Using the notation of Lemma 1 and 2, matrices $\mathbf{A} - \mathbf{B}$ and $\Sigma(\mathbf{A}) - \Sigma(\mathbf{B})$ have the decreasingly ordered singular values $\sigma_1(\mathbf{A} - \mathbf{B}) \geq \dots \geq \sigma_q(\mathbf{A} - \mathbf{B})$ and $s_{[1]}(\mathbf{A}, \mathbf{B}) \geq \dots \geq s_{[q]}(\mathbf{A}, \mathbf{B})$. Then we have

$$N_k(\mathbf{A} - \mathbf{B}) = \sum_{i=1}^k \sigma_i(\mathbf{A} - \mathbf{B}) \geq \sum_{i=1}^k s_{[i]}(\mathbf{A}, \mathbf{B}) = N_k(\Sigma(\mathbf{A}) - \Sigma(\mathbf{B})), \quad (8)$$

where the inequality is obtain by Lemma 1. The Lemma 2 implies (8) is equivalent to $\|\mathbf{A} - \mathbf{B}\| \geq \|\Sigma(\mathbf{A}) - \Sigma(\mathbf{B})\|$ for every unitarily invariant norm $\|\cdot\|$. \blacksquare

Then we give the proof of Theorem 1.

Proof Using the notation of above lemmas, we can bound the objective function as follow. For any $\mathbf{C} \in \mathbb{R}^{d \times k}$ and $\delta \in \mathbb{R}$, we have

$$\begin{aligned} & \|\mathbf{M} - \mathbf{C}\mathbf{C}^\top - \delta\mathbf{I}\|_2 \\ & \geq \|\Sigma(\mathbf{M}) - \Sigma(\mathbf{C}\mathbf{C}^\top + \delta\mathbf{I})\|_2 \\ & = \max_{i \in \{1, \dots, d\}} |\sigma_i(\mathbf{M}) - \sigma_i(\mathbf{C}\mathbf{C}^\top) - \delta| \\ & \geq \max_{i \in \{k+1, \dots, d\}} |\sigma_i(\mathbf{M}) - \sigma_i(\mathbf{C}\mathbf{C}^\top) - \delta| \\ & = \max_{i \in \{k+1, \dots, d\}} |\sigma_i(\mathbf{M}) - \delta| \\ & \geq \max_{i \in \{k+1, \dots, d\}} |\sigma_i(\mathbf{M}) - \hat{\delta}|. \end{aligned}$$

The first inequality is obtained by Lemma 3 since the spectral norm is unitarily invariant, and the second inequality is the property of maximization operator. The last inequality can be checked easily by the property of medium and the equivalence of SVD and eigenvector decomposition for positive semi-definite matrix.

The first equality is based on the definition of spectral norm. The second equality holds due to the fact $\text{rank}(\mathbf{C}\mathbf{C}^\top) \leq k$ which leads $\sigma_i(\mathbf{C}\mathbf{C}^\top) = 0$ for any $i > k$.

Note that all above equalities occurs for $\mathbf{C} = \hat{\mathbf{C}}$ and $\delta = \hat{\delta}$. Hence we prove the result of this theorem. \blacksquare

We also demonstrate the similar result with respect to Frobenius norm in Corollary 1. This analysis includes the global optimality of the problem, while Zhang [13]'s analysis only prove the solution is local optimal. Additionally, our proof is more concise.

Corollary 1 Using the same notation of Theorem 1, we have the pair $(\tilde{\mathbf{C}}, \tilde{\delta})$ defined as

$$\tilde{\mathbf{C}} = \mathbf{U}_k(\boldsymbol{\Sigma}_k - \tilde{\delta}\mathbf{I})^{1/2}\mathbf{V} \quad \text{and} \quad \tilde{\delta} = \frac{1}{d-k} \sum_{i=j+1}^d \sigma_i$$

is the global minimizer of

$$\min_{\mathbf{C} \in \mathbb{R}^{d \times k}, \delta \in \mathbb{R}} \|\mathbf{M} - \mathbf{C}\mathbf{C}^\top - \delta\mathbf{I}\|_F^2,$$

where \mathbf{V} is an arbitrary $k \times k$ orthogonal matrix.

Proof We have the result similarly to Theorem 1.

$$\begin{aligned} & \|\mathbf{M} - \mathbf{C}\mathbf{C}^\top - \delta\mathbf{I}\|_F^2 \\ & \geq \|\boldsymbol{\Sigma}(\mathbf{M}) - \boldsymbol{\Sigma}(\mathbf{C}\mathbf{C}^\top + \delta\mathbf{I})\|_F^2 \\ & = \sum_{i=1}^d (\sigma_i(\mathbf{M}) - \sigma_i(\mathbf{C}\mathbf{C}^\top) - \delta)^2 \\ & \geq \sum_{i=k+1}^d (\sigma_i(\mathbf{M}) - \sigma_i(\mathbf{C}\mathbf{C}^\top) - \delta)^2 \\ & = \sum_{i=k+1}^d (\sigma_i(\mathbf{M}) - \delta)^2 \\ & \geq \sum_{i=k+1}^d (\sigma_i(\mathbf{M}) - \tilde{\delta})^2 \end{aligned}$$

The first four steps are similar to the ones of Theorem 1, but replace the spectral norm and absolute operator with Frobenius norm and square function. The last step comes from the property of the mean value.

We can check that all above equalities occurs for $\mathbf{C} = \tilde{\mathbf{C}}$ and $\delta = \tilde{\delta}$, which completes the proof.

■

Appendix B: The Proof of Theorem 2

Proof The Algorithm 3 implies the singular values of $\alpha^{(t-1)}\mathbf{I} + (\mathbf{B}^{(t-1)})^\top \mathbf{B}^{(t-1)}$ are

$$(\sigma_1^{(t)})^2 + \alpha^{(t-1)} \geq \dots \geq (\sigma_m^{(t)})^2 + \alpha^{(t-1)} \geq \alpha^{(t-1)} = \dots = \alpha^{(t-1)}.$$

Then we can use the Theorem 1 by taking

$$\mathbf{M} = \alpha^{(t-1)}\mathbf{I} + (\mathbf{B}^{(t-1)})^\top \mathbf{B}^{(t-1)},$$

$$\begin{aligned}\hat{\mathbf{C}} &= (\mathbf{V}^{(t-1)})^\top \sqrt{(\boldsymbol{\Sigma}^{(t-1)})^2 - (\sigma_m^{(t-1)})^2 \mathbf{I}} = (\mathbf{B}^{(t)})^\top, \\ \hat{\delta} &= [(\sigma_m^{(t-1)})^2 + \alpha^{(t-1)} + \alpha^{(t-1)}] / 2 = \alpha^{(t)}.\end{aligned}$$

Due to the last column of $\mathbf{B}^{(t)}$ is zero and $(\tilde{\mathbf{B}}^{(t)})^\top \tilde{\mathbf{B}} = (\mathbf{B}^{(t)})^\top \mathbf{B}^{(t)}$, we have $(\tilde{\mathbf{B}}^{(t)}, \alpha^{(t)})$ is the minimizer of the problem. \blacksquare

Appendix C: The Proof of Theorem 3

Proof In this proof, the notation $\mathbf{B}^{(t)}$ refer to the matrix obtain by the line 5 of Algorithm 3 at t -th iteration, and $\mathbf{B}^{(t)}$ is the same one for $(t-1)$ -th iteration (without inserting $\mathbf{a}^{(t)}$). In other words, we have $\mathbf{V}^{(t-1)}(\boldsymbol{\Sigma}^{(t-1)})^2 \mathbf{V}^{(t-1)} = (\mathbf{B}^{(t-1)})^\top \mathbf{B}^{(t-1)} + \mathbf{a}^{(t)}(\mathbf{a}^{(t)})^\top$. Then we can deserve the lower bound as follow

$$\begin{aligned}& \|\mathbf{A}^\top \mathbf{A} - (\mathbf{B}^\top \mathbf{B} + \lambda \mathbf{I})\|_2 \\ &= \left\| \sum_{t=1}^T \left[(\mathbf{a}^{(t)})^\top \mathbf{a}^{(t)} - (\mathbf{B}^{(t)})^\top \mathbf{B}^{(t)} + (\mathbf{B}^{(t-1)})^\top \mathbf{B}^{(t-1)} - \frac{1}{2}(\sigma_m^{(t-1)})^2 \mathbf{I} \right] \right\|_2 \\ &\leq \sum_{t=1}^T \left\| (\mathbf{a}^{(t)})^\top \mathbf{a}^{(t)} - (\mathbf{B}^{(t)})^\top \mathbf{B}^{(t)} + (\mathbf{B}^{(t-1)})^\top \mathbf{B}^{(t-1)} - \frac{1}{2}(\sigma_m^{(t-1)})^2 \mathbf{I} \right\|_2 \\ &= \sum_{t=1}^T \left\| \mathbf{V}^{(t-1)}(\boldsymbol{\Sigma}^{(t-1)})^2 (\mathbf{V}^{(t-1)})^\top - \mathbf{V}^{(t-1)}[(\boldsymbol{\Sigma}^{(t-1)})^2 - (\sigma_m^{(t-1)})^2 \mathbf{I}] (\mathbf{V}^{(t-1)})^\top - \frac{1}{2}(\sigma_m^{(t-1)})^2 \mathbf{I} \right\|_2 \\ &= \sum_{t=1}^T \left\| (\sigma_m^{(t-1)})^2 \mathbf{V}^{(t-1)} (\mathbf{V}^{(t-1)})^\top - \frac{1}{2}(\sigma_m^{(t-1)})^2 \mathbf{I} \right\|_2 \\ &= \frac{1}{2} \sum_{t=1}^T (\sigma_m^{(t-1)})^2 \leq \frac{1}{2(m-k)} \|\mathbf{A} - \mathbf{A}_k\|_F^2.\end{aligned}$$

The first three equalities are direct from the procedure of the algorithm, and the last one is due to $\mathbf{V}^{(t-1)}$ is column orthonormal. The first inequality comes from the triangle inequality of spectral norm. The last one can be obtain by the properties of (4). \blacksquare

Appendix D: The Proof of Theorem 4

Proof We can compare $\kappa(\mathbf{M}_{\text{RFD}})$ and $\kappa(\mathbf{M}_{\text{FD}})$ by the fact $\alpha \geq \alpha_0$ as follow

$$\kappa(\mathbf{M}_{\text{RFD}}) = \frac{\sigma_{\max}(\mathbf{B}^\top \mathbf{B}) + \alpha}{\alpha} \leq \frac{\sigma_{\max}(\mathbf{B}^\top \mathbf{B}) + \alpha_0}{\alpha_0} = \kappa(\mathbf{M}_{\text{FD}}).$$

The other inequality can be derived as

$$\kappa(\mathbf{M}_{\text{RFD}}) = \frac{\sigma_{\max}(\mathbf{B}^\top \mathbf{B}) + \alpha}{\alpha} \leq \frac{\sigma_{\max}(\mathbf{A}^\top \mathbf{A}) + \alpha}{\alpha} \leq \frac{\sigma_{\max}(\mathbf{A}^\top \mathbf{A}) + \alpha_0}{\alpha_0} = \kappa(\mathbf{M}),$$

where the first inequality comes from (3) and the others are easy to obtain. \blacksquare

Appendix E: The Proof of Theorem 5

Proof Suppose that $\mathbf{V}_\perp^{(t)}$ is the orthogonal complement of $\mathbf{V}^{(t)}$'s column space, that is $\mathbf{V}^{(t)}(\mathbf{V}^{(t)})^\top + \mathbf{V}_\perp^{(t)}(\mathbf{V}_\perp^{(t)})^\top = \mathbf{I}$, then we have

$$\begin{aligned}
 & \mathbf{H}^{(t)} - \mathbf{H}^{(t-1)} \\
 &= \alpha^{(t)}\mathbf{I} + (\mathbf{B}^{(t)})^\top \mathbf{B}^{(t)} - \alpha^{(t-1)}\mathbf{I} - (\mathbf{B}^{(t-1)})^\top \mathbf{B}^{(t-1)} \\
 &= \frac{1}{2}(\sigma_m^{(t-1)})^2\mathbf{I} - (\sigma_m^{(t-1)})^2\mathbf{V}^{(t-1)}(\mathbf{V}^{(t-1)})^\top + (\mu_t + \eta_t)\mathbf{g}^{(t)}(\mathbf{g}^{(t)})^\top \\
 &= \frac{1}{2}(\sigma_m^{(t-1)})^2[\mathbf{V}_\perp^{(t-1)}(\mathbf{V}_\perp^{(t-1)})^\top - \mathbf{V}^{(t-1)}(\mathbf{V}^{(t-1)})^\top] + (\mu_t + \eta_t)\mathbf{g}^{(t)}(\mathbf{g}^{(t)})^\top. \tag{9}
 \end{aligned}$$

By the proof of Theorem 2 in [4], we have

$$2R_T(\mathbf{w}) \leq \alpha_0\|\mathbf{w}\|^2 + R_G + R_D,$$

where

$$R_G = \sum_{t=1}^T (\mathbf{g}^{(t)})^\top (\mathbf{H}^{(t)})^{-1} \mathbf{g}^{(t)},$$

and

$$R_D = \sum_{t=1}^T (\mathbf{w}^{(t)} - \mathbf{w})^\top [\mathbf{H}^{(t)} - \mathbf{H}^{(t-1)} - \mu_t \mathbf{g}^{(t)}(\mathbf{g}^{(t)})^\top] (\mathbf{w}^{(t)} - \mathbf{w}).$$

We can bound R_G as follow

$$\begin{aligned}
 & \sum_{t=1}^T (\mathbf{g}^{(t)})^\top (\mathbf{H}^{(t)})^{-1} \mathbf{g}^{(t)} \\
 &= \sum_{t=1}^T \langle (\mathbf{H}^{(t)})^{-1}, \mathbf{g}^{(t)}(\mathbf{g}^{(t)})^\top \rangle \\
 &= \sum_{t=1}^T \frac{1}{\mu_t + \eta_t} \langle (\mathbf{H}^{(t)})^{-1}, \mathbf{H}^{(t)} - \mathbf{H}^{(t-1)} + \frac{1}{2}(\sigma_m^{(t-1)})^2[\mathbf{V}_\perp^{(t-1)}(\mathbf{V}_\perp^{(t-1)})^\top - \mathbf{V}^{(t-1)}(\mathbf{V}^{(t-1)})^\top] \rangle \\
 &\leq \frac{1}{\mu + \eta_T} \sum_{t=1}^T \langle (\mathbf{H}^{(t)})^{-1}, \mathbf{H}^{(t)} - \mathbf{H}^{(t-1)} + \frac{1}{2}(\sigma_m^{(t-1)})^2\mathbf{V}^{(t-1)}(\mathbf{V}^{(t-1)})^\top \rangle \\
 &= \frac{1}{\mu + \eta_T} \sum_{t=1}^T \left[\langle (\mathbf{H}^{(t)})^{-1}, \mathbf{H}^{(t)} - \mathbf{H}^{(t-1)} \rangle + \frac{1}{2}(\sigma_m^{(t-1)})^2 \text{tr}(\mathbf{V}^{(t-1)}(\mathbf{H}^{(t)})^{-1}(\mathbf{V}^{(t-1)})^\top) \right].
 \end{aligned}$$

The above equalities come from the properties of trace operator and (9) and the inequality is due to η_t is increasing.

The term $\sum_{t=1}^T \langle (\mathbf{H}^{(t)})^{-1}, \mathbf{H}^{(t)} - \mathbf{H}^{(t-1)} \rangle$ can be bound as

$$\begin{aligned}
 & \sum_{t=1}^T \langle (\mathbf{H}^{(t)})^{-1}, \mathbf{H}^{(t)} - \mathbf{H}^{(t-1)} \rangle \\
 & \leq \sum_{t=1}^T \ln \frac{\det(\mathbf{H}^{(t)})}{\det(\mathbf{H}^{(t-1)})} = \ln \frac{\det(\mathbf{H}^{(T)})}{\det(\mathbf{H}^{(0)})} \\
 & = \ln \frac{\prod_{i=1}^d \sigma_i(\mathbf{H}^{(T)})}{\alpha_0} \\
 & = \sum_{i=1}^d \ln \frac{\sigma_i((\mathbf{B}^{(T)})^\top \mathbf{B}^{(T)}) + \alpha^{(T)}}{\alpha_0} \\
 & = \sum_{i=1}^m \ln \frac{\sigma_i((\mathbf{B}^{(T)})^\top \mathbf{B}^{(T)}) + \alpha^{(T)}}{\alpha_0} + (d-m) \ln \frac{\alpha^{(T)}}{\alpha_0} \\
 & \leq m \ln \frac{\sum_{i=1}^m [\sigma_i((\mathbf{B}^{(T)})^\top \mathbf{B}^{(T)}) + \alpha^{(T)}]}{m\alpha_0} + (d-m) \ln \frac{\alpha^{(T)}}{\alpha_0} \\
 & = m \ln \left(\text{tr}((\mathbf{B}^{(T)})^\top \mathbf{B}^{(T)}) + \frac{\alpha^{(T)}}{\alpha_0} \right) + (d-m) \ln \frac{\alpha^{(T)}}{\alpha_0}.
 \end{aligned}$$

The first inequality is obtain by the concavity of the log determinant function, the second inequality comes from the Jensen's inequality and the other steps is based on the procedure of the algorithm.

The other one $\frac{1}{2} \sum_{t=1}^T (\sigma_m^{(t)})^2 \text{tr}(\mathbf{V}^{(t)} (\mathbf{H}^{(t)})^{-1} (\mathbf{V}^{(t)})^\top)$ can be bounded as

$$\begin{aligned}
 & \frac{1}{2} \sum_{t=1}^T (\sigma_m^{(t)})^2 \text{tr}(\mathbf{V}^{(t)} (\mathbf{H}^{(t)})^{-1} (\mathbf{V}^{(t)})^\top) \\
 & \leq \frac{1}{2} \sum_{t=1}^T \frac{(\sigma_m^{(t)})^2}{\alpha^{(t)}} \text{tr}(\mathbf{V}^{(t)} (\mathbf{V}^{(t)})^\top) \\
 & = \frac{m}{2} \sum_{t=1}^T \frac{(\sigma_m^{(t)})^2}{\alpha^{(t)}}. \tag{10}
 \end{aligned}$$

Hence, we have

$$R_G \leq \frac{1}{\mu + \eta_T} \left[m \ln \left(\text{tr}((\mathbf{B}^{(T)})^\top \mathbf{B}^{(T)}) + \frac{\alpha^{(T)}}{\alpha_0} \right) + (d-m) \ln \frac{\alpha^{(T)}}{\alpha_0} + \frac{m}{2} \sum_{t=1}^T \frac{(\sigma_m^{(t)})^2}{\alpha^{(t)}} \right]. \tag{11}$$

Then we bound the term R_D by using the fact (9) and Assumption 1 and 2.

$$\begin{aligned}
 R_D & = \sum_{t=1}^T (\mathbf{w}^{(t)} - \mathbf{w})^\top [\eta_t \mathbf{g}^{(t)} (\mathbf{g}^{(t)})^\top + \frac{1}{2} (\sigma_m^{(t-1)})^2 \mathbf{I} - \mathbf{V}^{(t-1)} (\mathbf{V}^{(t-1)})^\top] (\mathbf{w}^{(t)} - \mathbf{w}) \\
 & \leq \sum_{t=1}^T \eta_t (\mathbf{w}^{(t)} - \mathbf{w})^\top \mathbf{g}^{(t)} (\mathbf{g}^{(t)})^\top (\mathbf{w}^{(t)} - \mathbf{w}) + \frac{1}{2} \sum_{t=1}^T (\sigma_m^{(t-1)})^2 (\mathbf{w}^{(t)} - \mathbf{w})^\top (\mathbf{w}^{(t)} - \mathbf{w})
 \end{aligned}$$

$$\leq 4(CL)^2 \sum_{t=1}^T \eta_t + 2C^2 \sum_{t=1}^T (\sigma_m^{(t-1)})^2. \quad (12)$$

Finally, we obtain the result by combining (11) and (12). ■